RSC Advances

COMMUNICATION

View Article Online
View Journal | View Issue

Cite this: *RSC Adv.*, 2014, **4**, 39297

Received 19th June 2014
Accepted 12th August 2014

DOI: 10.1039/c4ra05937a

www.rsc.org/advances

Hydrothermal synthesis of single-crystalline mesoporous beta zeolite assisted by *N*-methyl-2-pyrrolidone†

Lijia Liu, Hongbin Wang, Runwei Wang, Shangjing Zeng, Ling Ni, Daliang Zhang, Liangkui Zhu, Houbing zou, Shilun Qiu and Zongtao Zhang*

Highly crystalline beta zeolite with large intracrystalline mesopores has been facilely synthesized *via* the introduction of low-cost *N*-methyl-2-pyrrolidone (NMP) into common TEAOH-based zeolite synthesis mixtures, which exhibited remarkably higher catalytic activity contrast than conventional porous catalysts (ZSM-5, beta and Al-MCM-41) in acid-catalyzed reactions involving large molecules.

Zeolites, with well-known physicochemical characteristics (*e.g.* individual micropores, large internal surface areas, strong acidity and high hydrothermal stability), have been successfully applied in separation, ion-exchange and catalysis.[1] In particular, the uniform micropore channels throughout the whole zeolite framework play an irreplaceable role in the shape-selective catalysis,[2] but simultaneously, also seriously limit their further applications in procedures involving bulky molecules.[3] Mesoporous materials with adjustable pore sizes of 2–50 nm (*e.g.* MCM-41, MCM-48, SBA-15 and SBA-1) may offer more accessible active sites in junction with faster mass transfer for effective conversion of large molecules.[4] Regrettably, these materials suffer from weak acidity and poor stability as a result of their intrinsic amorphous nature of pore walls.[5] Despite tremendous efforts, the optimized framework crystallinity is still far from those of crystalline zeolites.[6] More recently, mesoporous zeolites, with positive features of native microporous zeolites as well as mesoporous materials, have become a hot point in both scientific researches and industrial applications.[7] Several strategies, involving amphiphilic organosilanes,[8] cationic polymers,[9] inorganic nanoparticles[10] and post-treatments,[11] have been successfully developed for the synthesis of mesoporous zeolites. For instance, Ryoo's group developed a complicated amphiphilic organosilane featuring a long-chain alkylammonium moiety and a hydrolysable methoxysilyl group, with which they synthesized highly mesoporous zeolites with tunable mesopore structure.[6] Besides, Verboekend *et al.* successfully created large amounts of intracrystalline mesoporosity in bulk MFI zeolites by desilication treatment in alkaline medium followed by acid washing.[11a] With respect to these methods, the procedural complexity and/or economic feasibility may conflict with the modern industry expectations. In our previous work,[3a] we have reported, for the first time, a facile strategy for the synthesis of hierarchical ZSM-5 with house-of-cards-like (HCL) structure by addition of *N*-methyl-2-pyrrolidone (NMP) into a template-free zeolite synthesis system. The resulting HCL-ZSM-5 has large external surface and strong acidity, thus exhibiting remarkable catalytic performances in acid-catalyzed reactions concerning large molecules. Inspired by this finding, we sought to make further efforts to bring the NMP additive into common TEAOH-based alkaline beta zeolite synthesis mixtures, and study the impact of such kind of organics.

Mesoporous Beta (M-Beta) was hydrothermally synthesized from an aluminosilicate sol with a typical molar composition of $0.048Na_2O/0.023Al_2O_3/SiO_2/15.6H_2O/0.636$TEAOH/NMP. The relatively well-resolved X-ray diffraction (XRD) pattern in the 4–40° range can totally correspond to the characteristic peaks of Beta-type zeolite (Fig. 1A).[9b] As suggested by SEM and TEM images (Fig. 2), M-Beta presents a uniform dice-like morphology (300–350 nm), which consists of abundant highly crystalline nanocrystals (less than 30 nm). More interestingly, all these adjacent nanocrystals exhibit the consistent lattice fringes orientations over the entire TEM image region, meanwhile the selected area electron diffraction (SAED) pattern assigned to Beta-type zeolite structure shows highly discrete diffraction spots (Fig. 2D),[9b] demonstrating that dice-like M-Beta is complete a single crystal rather than random aggregation of nanocrystals. N_2 adsorption–desorption isotherms take on a typical type IV curve with a large H4 hysteresis loop (Fig. 1B), indicating a micro–meso hierarchical porous textural feature.

State Key Laboratory of Inorganic Synthesis and Preparative Chemistry, Jilin University, Changchun 130012, P. R. China. E-mail: zzhang@jlu.edu.cn; Fax: +86-431-85168115; Tel: +86-431-85168115

† Electronic Supplementary Information (ESI) available: Experimental and characterization details, XRD patterns, N_2 adsorption–desorption isotherms, SEM images, TEM images, SAED pattern, textural parameters of various catalysts. See DOI: 10.1039/c4ra05937a

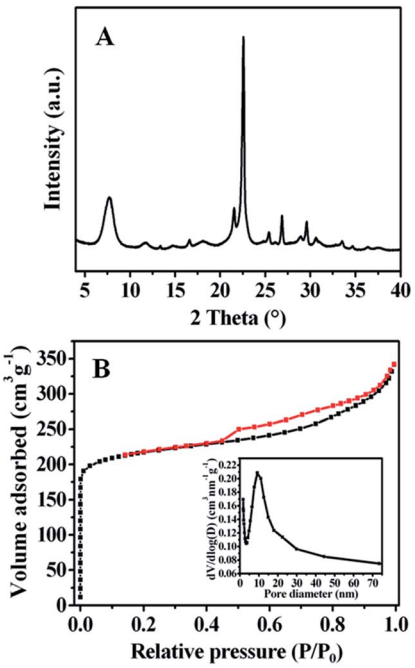

Fig. 1 (A) XRD pattern and (B) N_2 adsorption–desorption isotherms of M-Beta.

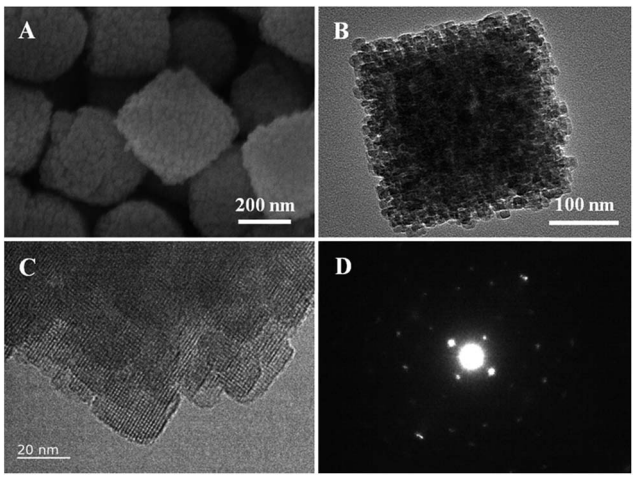

Fig. 2 (A) SEM image, (B) TEM image, (C) high resolution TEM image and (D) corresponding SAED pattern of M-Beta.

On the basis of Barrett–Joyner–Halenda (BJH) model, mesopore size distribution is centered at 9.2 nm (inset in Fig. 1B). The existence of such large mesopore in Beta zeolites would deservedly afford auxiliary benefits in catalysis. Calculated from the curve, the Brunauer–Emmett–Teller (BET) surface and total pore volume are 770 $m^2\ g^{-1}$ and 0.59 $cm^3\ g^{-1}$ respectively, among which, the micropore volume can reach as high as 0.28 $cm^3\ g^{-1}$, supporting that framework of M-Beta is fully crystallined. Besides, the external surface area is about 203 $m^2\ g^{-1}$ estimated by the *t*-plot method. It should be noted that intracrystalline mesopores cannot be achieved if NMP is absent in the starting aluminosilicate sol (Fig. S1–S3, ESI†). Taken together, these results confirm that NMP plays a critical role in the reasonable trade-off between the formation of mesoporous structure and the sacrifice of zeolite framework.

To gain deeper insights into the formation process of M-Beta, time-consumed tests were carried out (shown in Fig. S4–S6, ESI†). The visible Bragg diffraction firstly appeared after 3 hours of crystallization, and amorphous matrix together with some embedded ultra-small crystalline grains (nuclei) were clearly observed. With prolonged crystallization (6 h), these crystalline grains gradually grew into large quasi-spherical Beta crystals along with the consumption of surrounding amorphous gel agglomerates. Surprisingly, the crystals were totally dense single crystals, in which small wormlike intracrystalline mesopores existed. Further extending the reaction time to 12 h, the mesopores grew up and broke the Beta zeolite single crystal into small but continuous crystalline domains. However, the mesopores were still not rich enough, and the crystallinity of zeolite framework was somewhat poor, as suggested by TEM images. After cooling down and further recrystallizing for 48 h, highly crystalline dice-like Beta zeolite with large amounts of intracrystalline mesopores was fully formed. Throughout the whole crystallization process, there is no sign of an ordered assembly of preformed crystals, instead, classical "nucleation and dissolution-precipitation growth" model of hydrothermal crystallization is followed.[9b] Unlike to our previous study about HCL-ZSM-5,[3a] the evolution of M-Beta, typically in the mid- and late stage (after 6 h), behaves similar as a self-leaching process. As suggested by ICP test (Fig. S7, ESI†), the Si/Al ratios of resultant products take on an upward tendency with time extending. What is more, the Si/Al ratio of M-Beta sample is also slightly higher than that of conventional Beta. The phenomenon, strongly contradictory to the general principle of zeolites

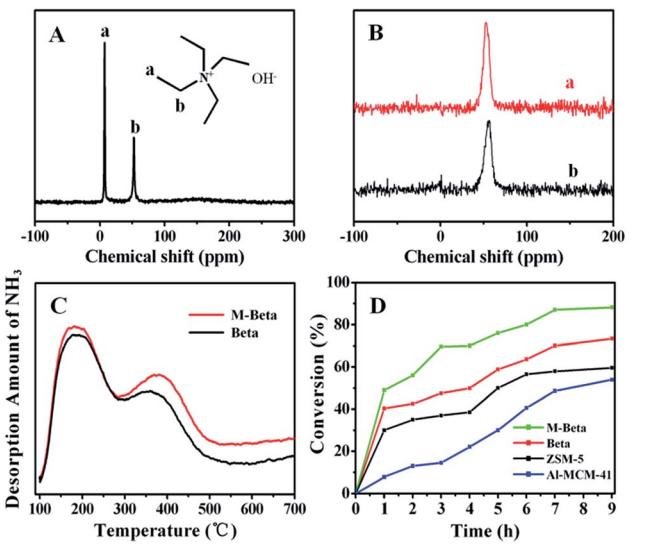

Fig. 3 (A) Solid-state ^{13}C NMR spectrum of uncalcined M-Beta. (B) Solid-state ^{27}Al NMR spectra of (a) uncalcined and (b) calcined M-Beta. (C) TPD-NH_3 curve of H form (red) M-Beta and (black) conventional Beta zeolite. (D) Performance comparison of M-Beta and conventional porous catalysts in the aldol condensation of benzaldehyde with *n*-butyl alcohol.

Table 1 Performance comparison of M-Beta and conventional porous catalysts in α-pinene isomerization[a]

Sample	Conversion (%)	Selectivity (%)					
		Camphene	Limonene	Terpinolene	α-Terpinene	γ-Terpinene	Others
ZSM-5	33.1	63.0	22.5	2.5	3.5	1.8	6.7
Beta	42.7	48.0	30.9	5.0	3.6	3.1	9.4
Al-MCM-41	97.4	44.6	27.5	10.7	9.0	3.9	4.3
M-Beta	98.6	44.9	23.4	10.0	11.2	5.5	5.0

[a] Reaction conditions: 70 °C, 30 min, 0.10 g of catalyst, 2.0 mL of α-pinene.

leaching in alkaline medium, however, may be interpreted as the realumination screening effect of organic pore-directing agents (PDAs), namely, suppressing realumination during desilication, as proposed by Verboekend *et al.*[11b] Besides, if the organic PDAs feature distinct affinity to the zeolite framework, the presence of such kind of organics would also enable better preserved intrinsic zeolite properties such as crystallinity and microporosity. Based on these theories, we conjecture that the strongly dipolar NMP molecules or their complex cations (*e.g.* $Na^+(NMP)_n$ or $TEA^+(NMP)_n$) may serve as so-called efficient PDAs that have great effects on the dissolution and recrystallization of aluminosilicates, allowing formation of highly crystalline Beta zeolite framework coupled with large intracrystalline mesopores. The solid-state ^{13}C NMR spectrum (Fig. 3A) of uncalcined M-Beta shows that only two resonance peaks attributed to the TEAOH appear. The lack of NMP characteristic peaks is likely due to the highly water-soluble property of NMP molecules.

The chemical activity of crystalline aluminosilicate zeolites is generally correlated to the coordination environment of aluminium atoms, which can be identified by ^{27}Al MAS-NMR.[3a] As shown in Fig. 3B, the as-synthesized M-Beta exhibits just one single resonance peak at about 53 ppm, assigned to tetrahedrally coordinated framework aluminium species, suggesting that all the Al atoms are located at intra-framework. After calcinations at 550 °C, an additional weak peak appears at around 0 ppm, assigned to octahedral extra-framework aluminium species, illustrating that slight dealumination occurs during the thermal treatment procedure. In addition, the acidity of M-Beta was also studied by a temperature-programmed desorption of NH_3 (TPD-NH_3) test. Typically, M-Beta shows a strong peak centered around 180 °C, associated with weak acidic sites, together with another peak centered around 380 °C, associated with medium-strong acidic sites, which is similar to that of conventional Beta zeolite (Fig. 3C and Table S2, ESI†). The above results reveal that most Al species in M-Beta framework are stable, and incorporation of mesopores hardly affects the intrinsic acidity of Beta zeolite.

The catalytic performance of M-Beta was initially tested in aldol condensation of benzaldehyde with *n*-butyl alcohol (Fig. 3D). Notably, M-Beta delivers a much higher conversion (88.2%) than those of conventional microporous catalysts (59.6% for ZSM-5 and 73.3% for Beta). The superior catalytic activity should be attributed to the presence of mesopores structures, which enables more accessible active sites as well as faster mass transfer of large molecules.[12] With respect to Al-MCM-41, the relatively weak acidity, arising from the amorphous nature of pore walls, is considered as the major reason of the lower conversion (53.8%).[12b] Moreover, the catalytic activity of M-Beta was further checked in α-pinene isomerisation. The total conversions of α-pinene along with the selectivities towards several major products (camphene, limonene, terpinolene, α-terpinene and γ-terpinene) are listed in Table 1. Obviously, conventional ZSM-5 and Beta zeolites exhibit relatively low conversions of 33.1% and 42.7% respectively, while our M-Beta affords the highest one of about 98.6%, which is very close to that of Al-MCM-41 (97.4%). The result can be easily explained by the fact that the isomerisation of α-pinene is a typical weak acid-catalyzed reaction, which could take place on both weak and strong acid sites.[13] Thus, molecular diffusion rather than the strength of acid sites becomes the key factor for the dominant of catalytic activity.

In summary, we have developed a feasible strategy for synthesizing single-crystalline mesoporous Beta zeolite by addition of low-cost NMP into a common TEAOH-based zeolite synthesis system. Importantly, the mesoporous Beta zeolite exhibits excellent catalytic properties in both weak (α-pinene isomerisation) and medium-strong (aldol condensation of benzaldehyde with *n*-butyl alcohol) acid-catalyzed reactions involving large molecules. This work, we think, may provide a reasonable train of thought for mass synthesis of highly active single-crystalline mesoporous zeolites, including but not limited to Beta, used for industrial catalysis.

Acknowledgements

This work was supported by the National Natural Science Foundation of China (20841003 and 20741001), and the New Century Outstanding Scholar Supporting Program.

Notes and references

1 K. Möller and T. Bein, *Chem. Soc. Rev.*, 2013, **42**, 3689.
2 (*a*) D. P. Serrano, J. Aguado, G. Morales, J. M. Rodríguez, A. Peral, M. Thommes, J. D. Epping and B. F. Chmelka, *Chem. Mater.*, 2009, **21**, 641; (*b*) R. Kore, R. Sridharkrishna and R. Srivastava, *RSC Adv.*, 2013, **3**, 1317.
3 (*a*) L. Liu, H. Wang, R. Wang, C. Sun, S. Zeng, S. Jiang, D. Zhang, L. Zhu and Z. Zhang, *RSC Adv.*, 2014, **4**, 21301;

(*b*) W. Chaikittisilp, Y. Suzuki, R. R. Mukti, T. Suzuki, K. Sugita, K. Itabashi, A. Shimojima and T. Okubo, *Angew. Chem., Int. Ed.*, 2013, **52**, 3355.

4 M.-J. Jeon, J.-K. Jeon, D. J. Suh, S. H. Park, Y. J. Sa, S. H. Joo and Y.-K. Park, *Catal. Today*, 2013, **204**, 170.

5 Z. Zhang, Y. Han, F. S. Xiao, S. Oiu, L. Zhu, R. Wang, Y. Yu, Z. Zhang, B. Zou, Y. Wang, H. Sun, D. Zhao and Y. Wei, *J. Am. Chem. Soc.*, 2001, **123**, 5014.

6 M. Choi, H. S. Cho, R. Srivastava, C. Venkatesan, D.-H. Choi and R. Ryoo, *Nat. Mater.*, 2006, **5**, 718.

7 (*a*) D. Nandan, S. K. Saxena and N. Viswanadham, *J. Mater. Chem. A*, 2014, **2**, 1054; (*b*) D. P. Serrano, J. M. Escola and P. Pizarro, *Chem. Soc. Rev.*, 2013, **42**, 4004.

8 A. Inayat, I. Knoke, E. Spiecker and W. Schwieger, *Angew. Chem., Int. Ed.*, 2012, **51**, 1962.

9 (*a*) R. Wang, W. Liu, S. Ding, Z. Zhang, J. Li and S. Qiu, *Chem. Commun.*, 2010, **46**, 7418; (*b*) J. Zhu, Y. Zhu, L. Zhu, M. Rigutto, A. van der Made, C. Yang, S. Pan, L. Wang, L. Zhu, Y. Jin, Q. Sun, Q. Wu, X. Meng, D. Zhang, Y. Han, J. Li, Y. Chu, A. Zheng, S. Qiu, X. Zheng and F.-S. Xiao, *J. Am. Chem. Soc.*, 2014, **136**, 2503.

10 (*a*) K. Na, W. Park, Y. Seo and R. Ryoo, *Chem. Mater.*, 2011, **23**, 1273; (*b*) K. Möller, B. Yilmaz, R. M. Jacubinas, U. Müller and T. Bein, *J. Am. Chem. Soc.*, 2011, **133**, 5284.

11 (*a*) D. Verboekend, S. Mitchell, M. Milina, J. C. Groen and J. Pérez-Ramírez, *J. Phys. Chem. C*, 2011, **115**, 14193; (*b*) D. Verboekend, G. Vilé and J. Pérez-Ramírez, *Cryst. Growth Des.*, 2012, **12**, 3123.

12 (*a*) J. Zhou, Z. Hua, J. Shi, Q. He, L. Guo and M. Ruan, *Chem.–Eur. J.*, 2009, **15**, 12949; (*b*) B. Liu, Y. Tan, Y. Ren, C. Li, H. Xi and Y. Qian, *J. Mater. Chem.*, 2012, **22**, 18631.

13 (*a*) A. Corma, *Chem. Rev.*, 2007, **107**, 2411; (*b*) Y. Wu, F. Tian, J. Liu, D. Song, C. Jia and Y. Chen, *Microporous Mesoporous Mater.*, 2012, **162**, 168.

